

# Research on Shear Lag Effect of T-shaped Short-leg Shear Wall

Chengqing Liu<sup>1,2,\*</sup>, Xiaodan Wei<sup>1,2</sup>, Handan Wu<sup>1,2</sup>, Qinfeng Li<sup>1,2</sup>,  
Xiangyong Ni<sup>1,2</sup>

RESEARCH ARTICLE

Received 17 May 2016; Revised 29 October 2016; Accepted 12 December 2016

## Abstract

*Longitudinal displacement of cross section of T-shaped short-leg shear wall was simplified to three parts: shear lag warping displacement, plane section bending displacement and axial displacement. Shear lag warping deformation was assumed as cubic parabola distribution along flange, and based on minimum potential energy principle, differential equations were deduced; with boundary conditions, a calculation theory for shear lag effect was established. With two T-shaped short-leg shear wall models, vertical stresses of flanges were obtained by calculation theory and finite element calculation respectively, and comparison between theoretical analysis results and numerical calculation results was made. At last, parameter analysis was carried out, and the influence of shear force, shear span ratio and height-thickness ratio on shear lag coefficient was obtained. Research shows that numerical calculation results are in good agreement with theoretical analysis results, and each parameter has different influence on shear lag coefficient.*

## Keywords

*T-shaped short-leg shear wall, minimum potential energy principle, shear lag effect, parameter analysis*

## 1 Introduction

As for components with box, T-shaped, I-shaped cross section, under the action of shear force, based on elementary theory of beam, it is known that normal stresses on cross section of the points with same vertical distance to neutral axis are the same. But in fact, when shear force flow passing from web to flange, due to the influence of shear deformation, normal stress distribution of flange is not homogeneous. At the same time, flat section assumption is no longer applicable and the greater distance from web, the corresponding normal stress is smaller. The shear wall with cross section height-thickness ratio between 4 to 8 is called as short-leg shear wall [1]. Under the action of axial force and horizontal force on T-shaped short-leg shear wall, the normal stress distribution of flange appears a phenomenon that the middle is bigger than the two sides. The shear lag phenomenon caused by shear deformation during shear force flow passing is referred to shear lag effect [2]. In the design, if shear lag effect is not considered enough, it may lead to transverse cracks on flange plate [3].

As a new structural component, T-shaped short-leg shear wall has been widely used in practical engineerings. At present, researches on short-leg shear wall are mainly focused on component tests and numerical analysis [4–7]. Common research methods for shear lag effect are energy variation method, analogy-bar method and numerical analysis method [8][9]. By assuming longitudinal displacement of T-shaped cross section and using variation principle, Zhang et al. deduced shear lag coefficient and deformation of component. In addition, under the conditions of various geometrical parameters and loading forms, the influence on shear lag effect and deformation was discussed. The deficiency of this study is that boundary conditions of shear wall are different from real situation [10]. Q. Z. Luo, Y. J. Chen presented analytical theory and computational method for thin-walled curved box girders in terms of shear lag effect and geometric nonlinearity. Based on potential variation principle and theory of thin-walled box girders, geometry nonlinear governing differential equations of thin-walled curved box girder considering the influence of shear lag effect of flange's stress and large deflection were established. The equations were solved by means of Newton-Raphson iteration method [11]. Shi

<sup>1</sup>School of civil engineering, Southwest JiaoTong University, Chengdu Sichuan 610031, China

<sup>2</sup>Key laboratory of high-speed railway engineering ministry of education, Chengdu Sichuan 610031, China

\*Corresponding author, email: [lcqj@163.com](mailto:lcqj@163.com)

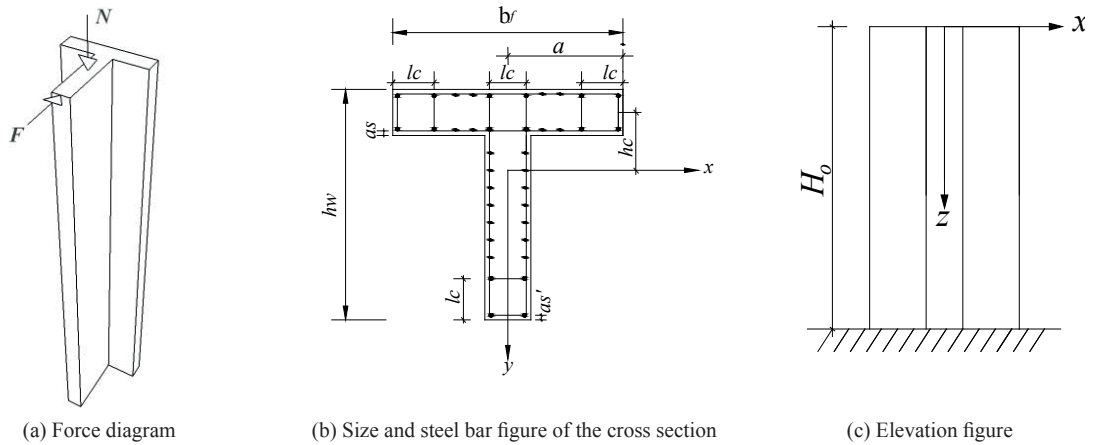


Fig. 1 Calculation diagrams of T-shaped short-leg shear wall

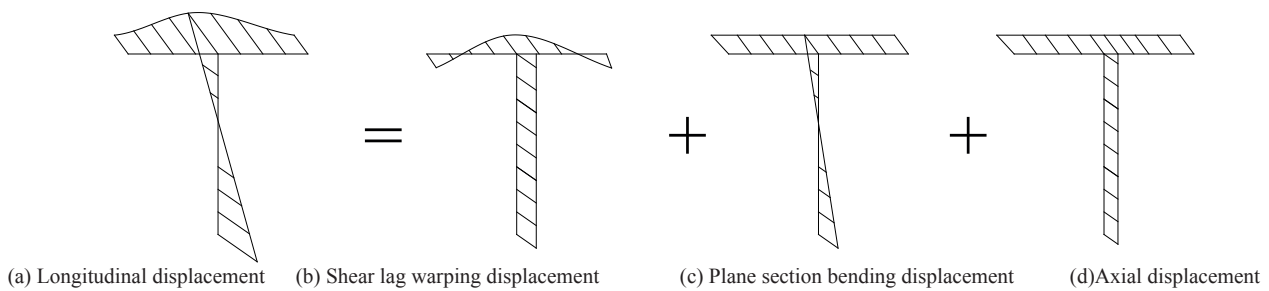


Fig. 2 Longitudinal displacement of the cross section

et al analyzed shear lag effect of T-shaped shear wall with flange by finite element software and discussed the influence of different design parameters on shear lag effect. Finally, according to the stress equivalent principle, the effective flange width values were obtained under different working conditions [12]. This paper is to establish a calculation theory for shear lag effect of T-shaped short-leg shear wall by energy vibration method of minimum potential theory, which considers the action of axial force, shear force and moment, and the validity of the theory was validated by finite element software. Finally, with shear lag effect calculation theory of T-shaped short-leg shear wall, the influence of shear force, shear span ratio and height-thickness ratio on shear lag coefficient was studied.

## 2 Total potential energy of T-shaped shear wall

### 2.1 Basic information

The shear force and axial force were both loading at the top of T-shaped short-leg shear wall, as shown in Fig. 1 (a). The axial force was simplified as equivalent uniform distributed load.

Fig. 1 (b) is the size of cross section and steel bar figure of T-shaped short-leg shear wall; In this figure,  $h_w$  is the height of cross section,  $b_f$  is the width of flange cross section,  $l_c$  is the length of edge constraint component,  $a_s$  and  $a_s'$  are flange and web longitudinal steel bar distance from concrete edge respectively.  $a = b_f/2$ . Fig. 1 (c) is an elevation figure of T-shaped short-leg shear wall. Axial direction of T-shaped short-leg shear wall is z axis direction and  $H_0$  is the height of T-shaped short-leg shear wall.

### 2.2 Calculation assumption

The energy variation method was used to study shear lag effect of T-shaped short-leg shear wall, and the following basic assumptions were introduced:

(1) Under the action of symmetrical horizontal load and axial load, the neutral axis location of cross section is calculated according to flat section assumption. Deformation of web is complied with flat section assumption. Longitudinal displacement function of flange plate is fitted by cubic parabola.

(2) When calculating the strain energy of flange plate, lateral strain, vertical strain and out-of-plane shear strain are very small and could be ignored, therefore, only the effect of  $\varepsilon_c$  and  $\gamma_{xz}$  are considered. Where  $\varepsilon_c$  is the axial strain of flange,  $\gamma_{xz}$  is the shear strain of flange.

### 2.3 Longitudinal displacement function

Based on the mechanical characteristics analysis of T-shaped short-leg shear wall, the longitudinal displacement of cross section was simplified to three parts: shear lag warping displacement, plane section bending displacement and axial displacement, as shown in Fig. 2. Shear lag warping displacement distribution curve was assumed as cubic parabola. Longitudinal displacement  $u(x,y,z)$  was expressed by two generalized displacements: vertical deflection  $\omega(z)$  and shear lag generalized displacement  $u(z)$ . So the expression of longitudinal displacement  $u(x,y,z)$  can be expressed as follows:

$$u(x, y, z) = -y\omega'(z) + f(x, y)u(z) + \frac{q}{E}(H_0 - z) \quad (1)$$

Where  $f(x, y)$  is shear lag warping displacement function,  $q$  is equivalent uniform distributed load of axial force, which can be calculated by Eq. (2). Reinforced concrete elastic modulus adopted equivalent elastic modulus, which can be calculated by Eq. (3).  $H_0$  is the height of T-shaped short-leg shear wall.

$$q = \frac{N}{A} \quad (2)$$

$$E = \frac{E_c A_c + E_{sw} A_{sw} + E_s A_s}{A} \quad (3)$$

Where  $E_c$  is the elastic modulus of concrete,  $A_c$  is the cross section area of concrete,  $E_{sw}$  is the elastic modulus of vertical distribution steel bar,  $A_{sw}$  is the cross section area of vertical distribution steel bar,  $E_s$  is the elastic modulus of longitudinal steel bar,  $A_s$  is the cross section area of longitudinal steel bar,  $A$  is total cross section area. Because the flange plate is longer, the influence of shear lag effect needed to be considered. The longitudinal displacement  $u_c$  of flange plate can be expressed as follows:

$$u_c = h_c \left( \omega'(z) + \left[ 1 - \frac{(-x+a)^3}{a^3} \right] u(z) \right) + \frac{q}{E}(H_0 - z) \quad (4)$$

$(0 \leq x \leq a)$

Where  $h_c$  is the distance between central axis and coordinate axis, because the web is narrow, the shear lag effect was not considered. The longitudinal displacement  $u_w$  of web can be expressed as follows:

$$u_w = -y_w \omega'(z) + \frac{q}{E}(H_0 - z) \quad (5)$$

Where  $y_w$  is the y-coordinate of web centroid.

## 2.4 Total potential energy expressions

The normal stress  $\sigma_c$  and shear stress  $\tau_c$  of flange plate can be expressed as follows:

$$\sigma_c = E \frac{\partial u}{\partial z} = Eh_c \left( \omega''(z) + \left[ 1 - \frac{(-x+a)^3}{a^3} \right] u'(z) \right) - q \quad (6)$$

$$\tau_c = G \frac{\partial u}{\partial x} = Gh_c \frac{3(-x+a)^2}{a^3} u(z) \quad (7)$$

Where  $G$  is the shear modulus of reinforced concrete materials,  $G = 0.4E$ . The strain energy  $U_c$  of concrete flange plate can be expressed as follows:

$$\begin{aligned} \delta \Pi = \int_0^{H_0} \left\{ \delta \omega''(z) \left( EI_c \omega''(z) + \frac{3}{4} EI_c u'(z) - qS_c + EI_w \omega''(z) + qS_w + M_z \right) + \right. \\ \left. \delta u'(z) \left[ -\frac{3}{4} qS_c + \frac{9}{14} EI_c u'_z + \frac{3}{4} EI_c \omega''(z) \right] + Gh_c^2 \frac{18b}{5a} u(z) \delta u(z) \right\} dz - \frac{3}{4} qS_c u(z) \Big|_{z=0} \end{aligned} \quad (14)$$

$$U_c = \frac{1}{2} \int_{V_c} (E\varepsilon_c^2 + G\tau_c^2) dv = \frac{1}{2} \int_{V_c} \left[ E \left( \frac{\partial u}{\partial z} \right)^2 + G \left( \frac{\partial u}{\partial x} \right)^2 \right] dv \quad (8)$$

Combined with Eq. (6), Eq. (7) and Eq. (8), Eq. (9) can be obtained:

$$\begin{aligned} U_c = \frac{1}{2} \int_0^{H_0} \left\{ \frac{1}{2} EI_c \left( [\omega''(z)]^2 + \frac{9}{14} (u'_z)^2 + \frac{3}{2} \omega''(z) u'(z) \right) + \right. \\ \left. Eab \left( \frac{q}{E_c} \right)^2 - qS_c \omega''(z) - \frac{3}{4} qS_c u'(z) + Gh_c^2 \frac{9b}{5a} [u(z)]^2 \right\} dz \end{aligned} \quad (9)$$

Where,  $I_c = 2h_c^2 ab$ ,  $S_c = 2h_c ab$ ,  $b$  is the thickness of T-shaped short-leg shear wall. Similarly, the strain energy  $U_w$  of web can be expressed as follows:

$$U_w = \frac{1}{2} EI_w \int_0^{H_0} [\omega''(z)]^2 dz + \frac{q^2}{2E} A_w H_0 + qS_w \int_0^{H_0} \omega''(z) dz \quad (10)$$

Where  $I_w$  is the inertia moment of web cross section to x axis,  $A_w$  is cross section area of the web,  $S_w$  is the static moment of web cross section to x axis. With the boundary conditions of T-shaped short-leg shear wall, external potential energy  $V_p$  can be expressed as follows:

$$V_p = \int_0^{H_0} M_z \omega''(z) dz - \int_A qu(x, y) \Big|_{z=0} dA \quad (11)$$

Where  $M_z$  is the moment on cross section with  $z$  coordinate. Based on Eq. (9), Eq. (10) and Eq. (11), the total potential energy  $\Pi$  of T-shaped short-leg shear wall can be expressed as follows:

$$\Pi = 2U_c + U_w + V_p \quad (12)$$

## 3 Building governing differential equations

Based on minimum potential energy principle, under the action of known force, the displacements which satisfy displacement boundary conditions make  $\Pi$  become the stationary value. When the system is in stable equilibrium state, the total potential energy  $\Pi$  is a minimum value. So the first variation of total potential energy  $\Pi$  equals to 0.

$$\delta \Pi = \delta(2U_c + U_w + V_p) = 0 \quad (13)$$

In conclusion, the first variation of total potential energy  $\Pi$  can be obtained: (Eq. 14)

$$\begin{aligned} \delta\Pi = \int_0^{H_0} & \left\{ \delta\omega''(z) \left( EI_c \omega''(z) + \frac{3}{4} EI_c u'(z) - qS_c + EI_w \omega''(z) + qS_w + M_z \right) \right. \\ & \left. + \delta u(z) \left[ -\frac{9}{14} EI_c u_z'' + Gh_c^2 \frac{18b}{5a} u(z) - \frac{3}{4} EI_c \omega'''(z) \right] \right\} dz \\ & + \delta u(z) \left[ -\frac{3}{4} qS_c + \frac{9}{14} EI_c u_z' + \frac{3}{4} EI_c \omega''(z) \right] \Big|_0^{H_0} - \frac{3}{4} qS_c u(z) \Big|_{z=0} \end{aligned} \quad (15)$$

The first variation of total potential energy  $\Pi$  was changed into: (Eq. 15)

The governing differential equations can be obtained:

$$EI_c \omega''(z) + \frac{3}{4} EI_c u'(z) - qS_c + EI_w \omega''(z) + qS_w + M_z = 0 \quad (16)$$

$$-\frac{9}{14} EI_c u_z'' + Gh_c^2 \frac{18b}{5a} u(z) - \frac{3}{4} EI_c \omega'''(z) = 0 \quad (17)$$

Forced boundary conditions can be expressed as follows:

$$\delta u(z) \left[ -\frac{3}{4} qS_c + \frac{9}{14} EI_c u_z' + \frac{3}{4} EI_c \omega''(z) \right] \Big|_0^{H_0} - \frac{3}{4} qS_c u(z) \Big|_{z=0} = 0 \quad (18)$$

Organized Eq. (16) and Eq. (17), the governing differential equations of generalized displacement can be expressed as follows:

$$u_z'' - k^2 u(z) = -\frac{28F}{3E(I_c + 8I_w)} \quad (19)$$

In Eq. (19),  $k = \sqrt{\frac{112(I_c + I_w)G}{5Ea^2(I_c + 8I_w)}}$ ,  $Q(z)$  is the shear force of

T-shaped short-leg shear wall. According to the mechanical boundary condition:

$$Q(z) = F \quad (20)$$

The general solution of generalized displacement is as follows:

$$u(z) = C_1 \sinh(kz) + C_2 \cosh(kz) + \frac{28F}{3E(I_c + 8I_w)k^2} \quad (21)$$

## 4 Stress expressions

### 4.1 The boundary conditions

According to Eq. (1), the equation  $u(x, y, z) \Big|_{z=H_0} = 0$  can be deduced. Because the bottom of shear wall was fixed, namely  $\omega'(z) \Big|_{z=H_0} = 0$ , the displacement boundary conditions of  $u(z)$  can be obtained:

$$u(z) \Big|_{z=H_0} = 0 \quad (22)$$

$$\delta u(z) \Big|_{z=H_0} = 0 \quad (23)$$

Owing to the arbitrary of  $\delta u(z) \Big|_{z=0}$ , Eq. (18) can be expressed as:

$$\frac{9}{7} Eh_c^2 abu_z' + \frac{3}{2} Eh_c^2 ab\omega''(z) \Big|_{z=0} = 0 \quad (24)$$

With the known condition:  $qS_w - 2qh_c ab = 0$ ,  $\omega''(z)$  can be obtained by Eq. (16) and Eq. (17):

$$\omega''(z) = \frac{Fz}{E(I_c + I_w)} - \frac{3Eh_c^2 ab}{2E(I_c + I_w)} [kC_1 \cosh(kz) + kC_2 \sinh(kz)] \quad (25)$$

With Eq. (21):

$$u(z) \Big|_{z=H_0} = C_1 \sinh(kH_0) + C_2 \cosh(kH_0) - \frac{28F}{3E(I_c + 8I_w)k^2} = 0 \quad (26)$$

### 4.2 Stress expressions

Based on Eq. (24):

$$C_1 = 0 \quad (27)$$

With Eq. (26),  $C_2$  can be obtained:

$$C_2 = \frac{28F}{3E(I_c + 8I_w)k^2 \cosh(kH_0)} \quad (28)$$

The stress expression of flange can be expressed as follows:

$$\begin{aligned} \sigma_c(x, z) = & -E_c y_c \left( \omega''(z) + k \left[ 1 - \frac{(-x+a)^3}{a^3} \right] [C_1 \cosh(kz) + C_2 \sinh(kz)] \right) - q \\ & 0 \leq x \leq a \end{aligned} \quad (29)$$

The stress expression of web can be expressed as follows:

$$\sigma_w(x, z) = E_c y_w \omega''(z) - q \quad (30)$$

## 5 Example analysis

With the practical examples, the vertical stresses of flanges were obtained by the above calculation theory and finite element calculation software. The theoretical analysis and numerical calculation results were compared and analyzed.

### 5.1 Example case

Based on shear wall design specification [1], two T-shaped short-leg shear wall components were designed. The sizes of T-shaped short-leg shear walls and axial compression ratios are shown in Table 1.

**Table 1** Section size and axial compression ratio

Model	$b(\text{mm})$	$b_f(\text{mm})$	$h_w(\text{mm})$	$l_c(\text{mm})$	$a_s(\text{mm})$	$u_n(\text{N}/\text{N}=1)$
TS-1	200	1000	1000	200	20	0.1
TS-2	200	1600	1600	320	20	0.4

Where  $u_n$  is axial compression ratio.

The shear force of Model TS-1 is 80 kN and its shear span ratio is 3; The shear force of Model TS-2 is 150kN and its shear span ratio is 3. The longitudinal steel bar on cross section is HRB400; the horizontal and distributed steel bar is HRB335; the strength grade of concrete is C30. The steel bar information of T-shaped short-leg shear wall models by calculating, is shown as Table 2.

**Table 2** Steel bar information of T-shaped short-leg shear walls

Model	$A_s(\text{mm}^2)$	$A_s'(\text{mm}^2)$	$\rho_w(\%)$	Edge constraint component	Vertical and horizontal distributed steel bar
TS-1	1608	4824	0.30	8Φ16mm	Φ10mm@100mm
TS-2	1608	4824	0.35	8Φ16mm	Φ10mm@90mm

In Table 2, 8Φ16mm represents 8 steel bars of 16mm diameter; Φ10mm@100mm represents 10mm in diameter of the steel bars and 100mm in spacing.

## 5.2 Finite element analysis

### 5.2.1 Finite element modeling

SOLID65 was used to simulate the concrete. Because the top cross section of T-shaped short-leg shear wall model needed to be applied horizontal and vertical homogeneous load in finite element analysis calculation, SURF154 element was used. Multi-linear kinematic hardening model KINH was used for the concrete constitutive. The strength grade of concrete is C30 and the axial compressive strength characteristic value  $f_{ck}$  of concrete is 20.1N/mm<sup>2</sup>; the elastic modulus is  $E_c = 3.0e4 \text{ N}/\text{mm}^2$ ; the poisson's ratio is  $\nu = 0.2$ . According to concrete uniaxial compression stress-strain relationship in GB50010-2010 Concrete structure design code [1], the constitutive relation of concrete was simplified to 11 featuring points and shown as Fig. 3. Combined with experience value, shear transfer coefficient is  $\beta_t = 0.125$ ; shear transfer coefficient of closed crack is  $\beta_c = 0.95$ .

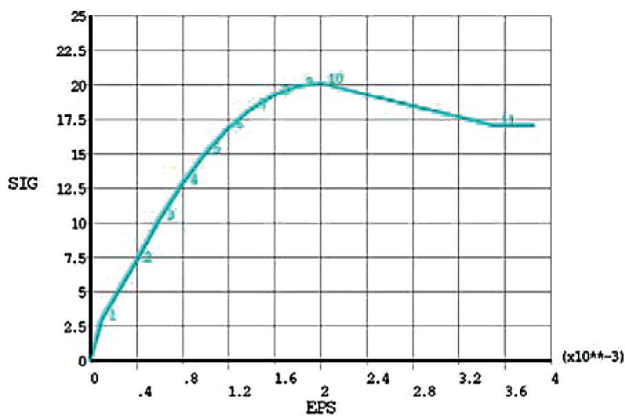


**Fig. 3** Constitutive relation of concrete

The ideal elastic-plastic model was adopted for constitutive relation of steel bar. The tensile strength of longitudinal steel bar is  $f_y = 360\text{N}/\text{mm}^2$  and its elastic modulus is  $E_s = 2.0e5 \text{ N}/\text{mm}^2$ ; the tensile strength of distributed steel bar is  $f_{yw} = 300\text{N}/\text{mm}^2$  and its elasticity modulus is  $E_{sw} = 2.0e5 \text{ N}/\text{mm}^2$ ; the poisson's ratio is  $\nu = 0.3$ .

### 5.2.2 Applying the boundary conditions

According to Fig. 1, Table 1 and Table 2, the finite element calculation model of T-shaped short-leg shear wall was established. Steel bar was added to finite element model by setting concrete real constant. There are three edge constraint components on flange, and there is an edge constraint component on web end. The grid size of finite element is 50mm, and the model includes 23280 elements. The finite element model is as shown in Fig. 4.

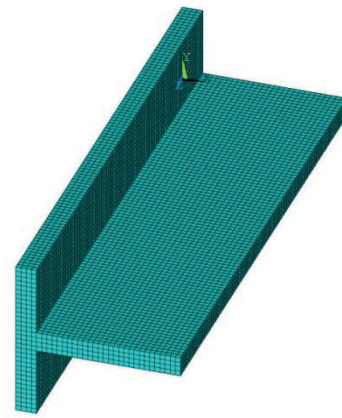


**Fig. 4** Finite element model of T-shaped short-leg shear wall

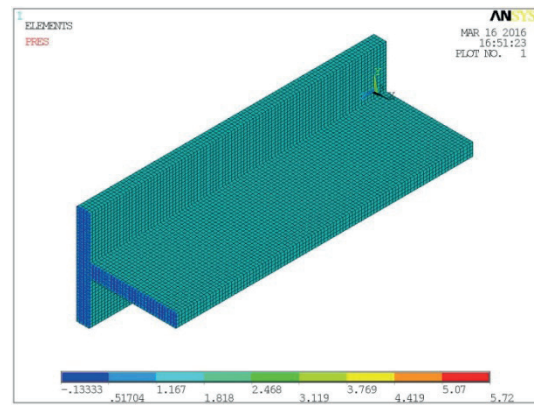


**Fig. 5** Load application

According to axial compression ratio and shear force of T-shaped short-leg shear wall, the corresponding uniform shear stress can be obtained, and the uniform shear stress was applied to top cross section by surface effect element. As shown in Fig. 5. To limit three free degrees of calculation model's bottom nodes, the bottom of T-shaped short-leg shear wall was fixed on foundation. As shown in Fig. 6.

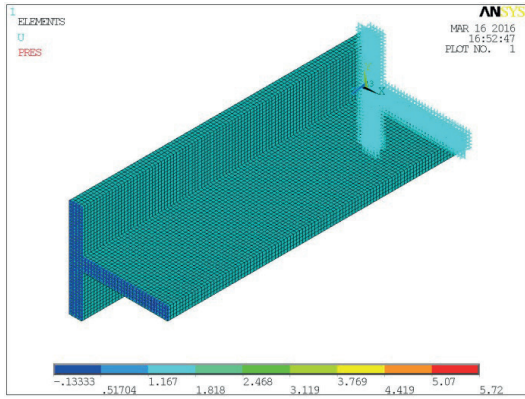


Fig. 6 Boundary conditions

### 5.2.3 Calculation results analysis

Under the action of axial force and shear force, the deformation diagram is as shown in Fig. 7. The bottom elements were selected to check the stress of z axis direction. The z axis direction stress is shown in Fig. 8.



Fig. 7 Deformation diagram

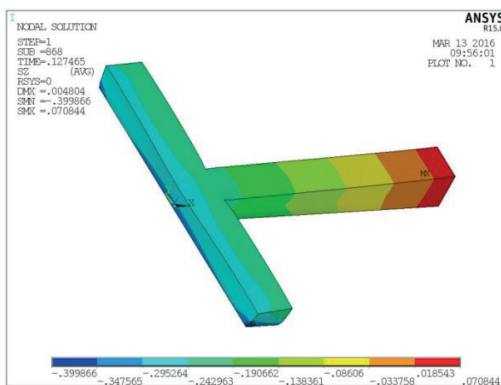


Fig. 8 Stress diagram

### 5.3 Comparison and analysis

Based on the above calculation theory and finite element numerical analysis, the axial stress distribution on flange plates of Model TS-1 and Model TS-2 are obtained. Due to the cross section and load are symmetrical, the axial stress distribution of flange plate whose x coordinate is in  $[0, \frac{b_f}{2}]$  is given. The comparison between theoretical analysis results and numerical calculation results was made, which is shown as in Fig. 9 and Fig. 10.

Under the action of axial force and shear force, the deformation diagram is as shown in Fig. 7. The bottom elements were selected to check the stress of z axis direction. The z axis direction stress is shown in Fig. 8.

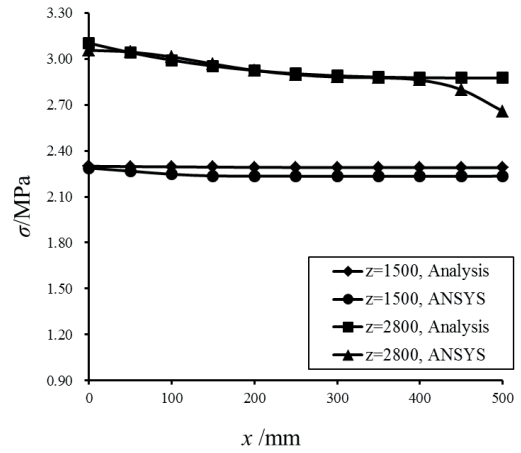


Fig. 9 Comparison between theoretical analysis and numerical calculation of flange plate axial stress of Model TS-1

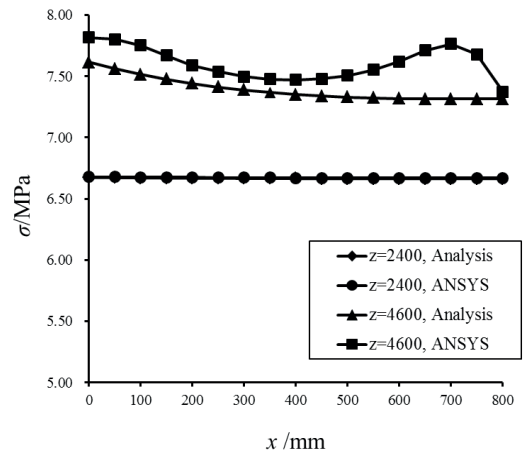


Fig. 10 Comparison between theoretical analysis and numerical calculation of flange axial stress of Model TS-2

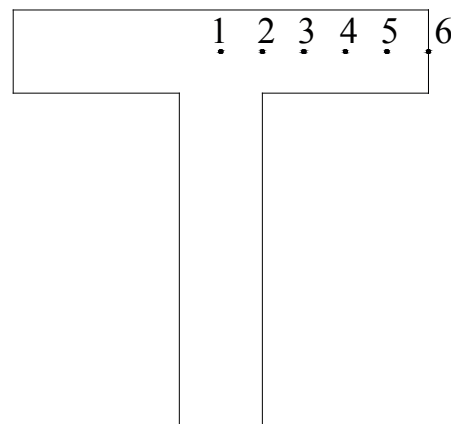


Fig. 11 Arrangement of measuring points on the cross section

Table 3 summarized the comparison between theoretical analysis values and numerical calculation values of the axial stress of measuring points in Fig. 11. The x coordinates of measuring points are shown as Table 4.

Fig. 9, Fig. 10 and Table 3 show that the numerical calculation values are in good agreement with theoretical analysis values, which suggests that the above calculation theory is reliable.

**Table 3** Comparison between theoretical analysis and numerical calculation of the axial stress of measuring points

Measuring points		1	2	3	4	5	6
Model TS-1	Z=2800mm Theoretical values	-3.1034	-2.9921	-2.9246	-2.8899	-2.8772	-2.8754
	Z=2800mm Numerical values	-3.0565	-3.0137	-2.9252	-2.8814	-2.8622	-2.6587
Model TS-2	Z=4600mm Theoretical values	-7.6142	-7.4747	-7.3867	-7.3384	-7.3179	-7.3132
	Z=4600mm Numerical values	-7.8166	-7.669	-7.4976	-7.4787	-7.6188	-7.3735

In Table 3, the unit of axial stress is N/mm<sup>2</sup>; “-” represents axial stress is compressive stress.

**Table 4** The x coordinates of measuring points

Measuring point	1	2	3	4	5	6
x coordinate	$\frac{b_f \times 0}{2}$	$\frac{b_f \times 1}{2 \times 5}$	$\frac{b_f \times 2}{2 \times 5}$	$\frac{b_f \times 3}{2 \times 5}$	$\frac{b_f \times 4}{2 \times 5}$	$\frac{b_f}{2}$

## 6 Parameter analyses

For the analyses of shear lag effect, shear lag coefficient is usually used to describe the influence degree, which can be obtained by following equation:

Where  $\sigma$  is the axial stress of flange plate with considering

$$\gamma = \frac{\sigma}{\bar{\sigma}} \quad (31)$$

shear lag effect,  $\bar{\sigma}$  is the flange plate axial stress with flat section assumption. Combined with mechanical characteristics of T-shaped short-leg shear wall,  $\bar{\sigma}$  can be calculated by the following equation:

Where  $I$  is the inertia moment to x axis of T-shaped short-leg shear wall cross section. The influence of shear force, axial force, shear span ratio and height-thickness ratio on shear lag coefficient of Model TS-1 and Model TS-2 was studied.

$$\bar{\sigma} = \frac{Fz}{I} y - q \quad (32)$$

leg shear wall cross section. The influence of shear force, axial force, shear span ratio and height-thickness ratio on shear lag coefficient of Model TS-1 and Model TS-2 was studied.

### 6.1 Influence of shear force on shear lag coefficient of T-shaped short-leg shear wall

Shear force is a fundamental factor to cause shear lag effect. In the above examples, keeping other parameters constant and only changing shear force, the influence of shear force on shear lag coefficient was researched. The distribution regularity of shear lag coefficient along x coordinate is shown as Fig. 12 and Fig. 13.

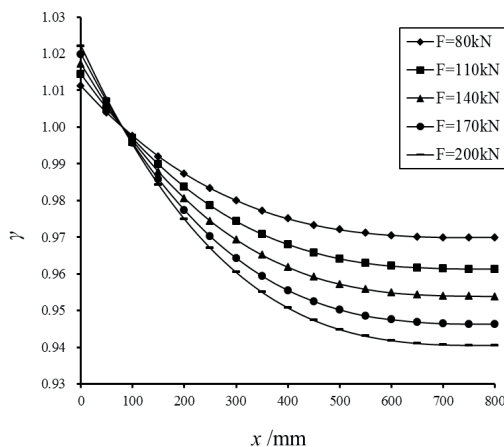


**Fig. 12** Influence of shear force on Model TS-1 shear lag coefficient

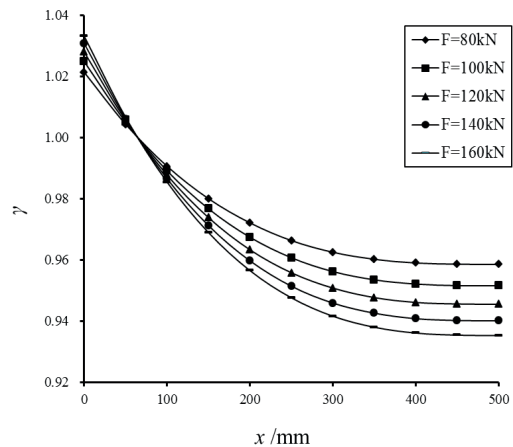


**Fig. 13** Influence of shear on Model TS-2 shear lag coefficient

In Fig. 12 and Fig. 13, the influence of shear force on shear lag coefficient keeps the same trend. The closer sectional flange is apart from web, the greater shear lag coefficient is, and the maximum shear lag coefficient is the center of flange section. Besides, the more heavily shear forces on model, the greater shear lag coefficient is.

### 6.2 Influence of shear span ratio on shear lag coefficient of T-shaped short-leg shear wall

Shear span ratio is an important parameter of shear wall. The distribution regularity of shear lag coefficient was studied when shear span ratios were equal to 2, 2.5, 3, 3.5, 4, respectively. The shear lag coefficient distribution regularity of the two models with the above shear span ratios is shown in Fig. 14 and Fig. 15.

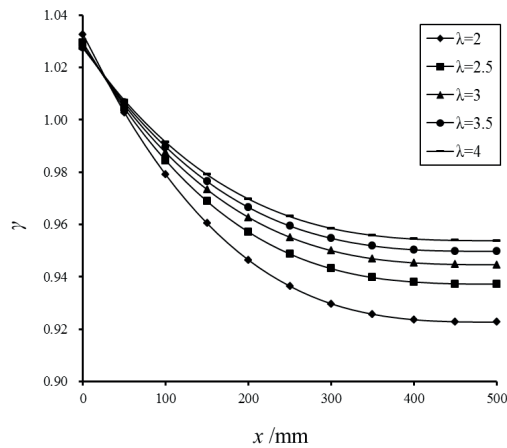


Fig. 14 Influence of shear span ratio on shear lag coefficient in Model TS-1

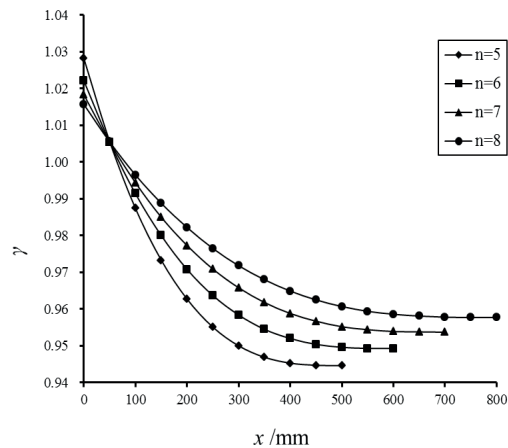


Fig. 16 Influence of height-thickness ratio on shear lag coefficient in Model TS-1

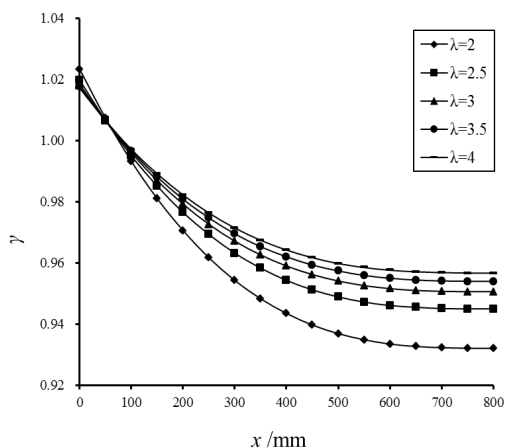


Fig. 15 Influence of shear span ratio on shear lag coefficient in Model TS-2

In Fig. 14 and Fig. 15, the shear lag coefficient distribution along x axis of the bottom section flange is more evenly with decrease of shear span ratio. And under the conditions of different shear span ratios, the maximum shear lag coefficients are almost same, which shows that the effect of shear span ratio on maximum shear lag coefficient is little.

### 6.3 Influence of height-thickness ratio on shear lag coefficient of T-shaped short-leg shear wall

The main difference between short-leg shear wall and general shear wall is height-thickness ratio of wall, and height-thickness ratio of short-leg shear wall is between 4 and 8. Height-thickness ratio is an important parameter, which influences mechanical characteristics and seismic performance of short-leg shear wall. Model TS-1 was used as an example to study the distribution regularity of shear lag coefficient of flange at the bottom section, and shear span ratios were set as 5,6,7,8, as shown in Fig. 16. In Fig.16, the bigger the height-thickness of wall limb cross section, the shear lag coefficient of bottom flange along x axis is more uniform and maximum shear lag coefficient is bigger which shows that shear span ratio has a significant influence on maximum shear lag coefficient.

## 7 Conclusions

(1) Longitudinal displacement of cross section was simplified to three parts: shear lag warping displacement, plane section bending displacement and axial displacement. Longitudinal displacement was represented by two generalized displacements: vertical deflection of component and shear lag generalized displacement. The total potential energy expression of T-shaped short-leg shear wall was obtained, and based on variation principle of minimum potential energy, with displacement and force boundary conditions, a shear lag effect theory of T-shaped short-leg shear wall was established.

(2) Combined with examples, the flange plate axial stress distribution of each model could be obtained by shear lag effect theory and finite element method, respectively. The theoretical calculation results and the numerical calculation results are in good agreement, which means that the shear lag effect theory is reliable.

(3) The shear lag effect theory of T-shaped short-leg shear wall in this paper was used for parameter analysis, and the influence of shear force, shear span ratio and height-thickness ratio of cross section on shear lag coefficient of T-shaped short-leg shear wall was obtained.

## Acknowledgments

This study is supported by the National Natural Science Foundation of China (No.51278428). The authors would like to express their gratitude to the National Natural Science Foundation of China.

## References

- [1] "GB 50010-2010. Code for Design of Concrete Structures." Construction industry press, Beijing. 2010.
- [2] Song, Q. G., Scordelis, A. C. "Shear-lag Analysis of T-, I-, and Box Beams." *Journal of Structural Engineering*. 116 (5), pp. 1290-1305. 1990. DOI: [10.1061/\(ASCE\)0733-9445\(1990\)116%3A5\(1290\)](https://doi.org/10.1061/(ASCE)0733-9445(1990)116%3A5(1290))
- [3] Luo, Q., Yu, J. "Problems of transverse cracking in flanges labs of reinforced concrete continuous box girder bridges." *Bridge Construction*. 117 (1), pp. 41-45. 1997.
- [4] Ding, J., Zhu, Y. "An elastic-plastic analysis of short-leg shear wall structures during earthquakes." *Earthquake Engineering and Engineering Vibration*. 11 (4), pp. 525-540. 2012. DOI: [10.1007/s11803-012-0139-8](https://doi.org/10.1007/s11803-012-0139-8)
- [5] Wu, Y., Kang, D., Yang, Y. B. "Seismic performance of steel and concrete composite shear wall with embedded steel truss for use in high-rise buildings." *Engineering Structures*. 125, pp. 39-53. 2016. DOI: [10.1016/j.engstruct.2016.06.050](https://doi.org/10.1016/j.engstruct.2016.06.050)
- [6] Wang, X., Su, Y., Yan, L. "Experimental and numerical study on steel reinforced high-strength concrete short-leg shear wall." *Journal of Constructional Steel Research*. 101, pp. 242-253. 2014. DOI: [10.1016/j.jcsr.2014.05.015](https://doi.org/10.1016/j.jcsr.2014.05.015)
- [7] Zhang, Y. H., Lin, L. X. "Shear lag analysis of thin-walled box girders based on a new generalized displacement." *Engineering Structures*. 61, pp. 73-83. 2014. DOI: [10.1016/j.engstruct.2013.12.031](https://doi.org/10.1016/j.engstruct.2013.12.031)
- [8] Reissner, E. "Analysis of shear lag in box beams by the principle of the minimum potential energy." *Quarterly of Applied Mathematics*. 4 (3). pp. 268-278. 1946. URL
- [9] Taherian, A. R., Evans, H. R. "The bar simulation method for the calculation of shear lag in multi-cell and continuous box girder." *Proceedings of the Institution of Mechanical Engineers. Part 2*, 63 (2), pp. 881-897. 1977. URL
- [10] Zhang, S., Li, Q., Guo, Z., Zhang, J. "Shear lag and effects of T-shaped short-leg shear wall." *Industrial Construction*. 44 (22), pp. 67-71. 2014.
- [11] Luo, Q. Z., Chen, Y. J. "Geometric nonlinear analysis of curved box continuous girders considering shear lag effect." *Advanced Materials Research*. Vols. 243-249, pp. 1811-1816, 2011. DOI: [10.4028/www.scientific.net/AMR.243-249.1811](https://doi.org/10.4028/www.scientific.net/AMR.243-249.1811)
- [12] Shi, Q., Wand, B., Zheng, X., Tian, J. "Shear lag effect analysis and effective flange width study of the T-shaped shear wall with flange." *Building Structure*. 44 (22). pp. 67-71. 2014.